Numerical analysis of the SEIR epidemic model with fractional order

Zain Ul Abadin Zafar[1], Sadaf Ijaz[1], and Cemil Tunc[2],*

[1]Department of Mathematics, University of Central Punjab, Lahore.

[2]Department of Mathematics, Faculty of Sciences, Van Yuzuncu Yil University, 65080, Campus, Van, Turkey.

Abstract

This study explores an SEIR epidemic model, aiming to achieve rapid stabilization of infectious disease dynamics. The model's dynamic behavior is analyzed with an emphasis on both local and global stability of equilibria using a Lyapunov function. The existence and uniqueness of the model are confirmed. The theoretical findings are validated, and the controller's effectiveness is illustrated through numerical simulations conducted in MATLAB/Simulink.

1. Introduction

Mathematical models are essential for developing preventive and control measures against epidemics. Research conducted by numerous scholars has established a robust scientific foundation for mitigating disease transmission through various protective measures, such as timely vaccination, mask-wearing [13], avoiding crowded areas [31], and voluntary quarantine [10]. By enhancing social awareness and decreasing individual infectivity, the spread of diseases can be significantly reduced. For example, Julien Arino and colleagues have developed a novel SEIAR model for influenza control through vaccination and antiviral treatment [4]. Similarly, Abbasi et al. introduced a prototype of SQEIAR models that focus on disease reduction through quarantine and optimal treatment of infected individuals, assuming balanced birth and death rates [1].

While complex models can correctly foretell the progression of an epidemic, simpler models are often more effective for forecasting the early stages of an epidemic. Nonetheless, all these models depend on predetermined factors related to infectivity during the latent period. In fact, factors like temperature and individual variations introduce random disturbances [18, 19, 32], which must be considered in disease spread prediction and control. Therefore, applying fractional order analysis to epidemic models is of significant practical importance. Some researchers have developed adequate conditions for the existence of global positive solutions by forming suitable Lyapunov functions [9].

This paper mainly aims to define local and global stability at equilibrium points and control the spread of epidemics under certain conditions. In section 1, a SEIR model is formulated as a fractional-order SEIR model. Section 2 explores the existence and uniqueness of positive solutions. Section 3 addresses the positivity of the invariant region. Section 4 defines local equilibrium stability and explains the basic reproductive number using the next-generation method. Section 5 explores global equilibrium stability through the construction of Lyapunov functions. Section 6 delves into parameter sensitivity. Section 7 explores the PRCC test for parameters. Section 8 outlines numerical schemes and simulations using MATLAB. The paper concludes with a summary and references.

2. Background Material

Definition 2.1. The fractional integral of order $\mathscr{B}$ for a function $\mathscr{Z}(\mathfrak{t})$ in Atangan-Baleanu-Caputo (ABC) sense is detailed as [3]:

$$^{\mathcal{ABC}}D_{\mathfrak{t}}^{-\mathscr{B}}(\mathscr{Z}(\mathfrak{t})) = \frac{1-\mathscr{B}}{\phi(\mathscr{B})}\mathscr{Z}(\mathfrak{t}) + \left[\frac{1}{\Gamma(\mathscr{B})\phi(\mathscr{B})}\right]\mathscr{B}\int_0^{\mathfrak{t}}(\mathfrak{t}-g)^{\mathscr{B}-1}\mathscr{Z}(g)dg. \tag{2.1}$$

Definition 2.2. The fractional derivative of order $\mathscr{B}$ for a function $\mathscr{Z}(\mathfrak{t})$ in Atangan-Baleanu-Caputo sense is detailed as [3]:

$$^{\mathcal{ABC}}D_{\mathfrak{t}}^{\mathscr{B}}(\mathscr{Z}(\mathfrak{t})) = \left[\frac{1}{1-\mathscr{B}}\right]\phi(\mathscr{B})\int_0^{\mathfrak{t}}\left[-\frac{\mathscr{B}E_{\mathscr{B}}}{1-\mathscr{B}}\right](\mathfrak{t}-g)^{\mathscr{B}}\mathscr{Z}'(g)dg. \tag{2.2}$$

Consider $\mathscr{B}$ in the semi open interval $(0,1]$, $\mathfrak{t}$ in the range $\mathfrak{t} \geq 0$, and $\mathfrak{t} < \infty$, and let $\mathscr{Z}$ be a differentiable function on $[0,\infty)$ such that $\mathscr{Z}' \in L^1(0,\infty)$. The Mittag-Leffler function $E_{\mathscr{B}}$ is defined as $E_{\mathscr{B}}(\mathfrak{t}) = \sum_{s=0}^{\infty}\frac{\mathfrak{t}^s}{\Gamma(s\mathscr{B}+1)}$. The normalization function $\phi(\mathscr{B})$ satisfies $\phi(0) = \phi(1) = 1$.

Definition 2.3. When applying the Laplace transform to the derivative of a function $\mathscr{N}(\mathfrak{t})$ in the Atangana-Baleanu-Caputo (ABC) sense, it is expressed as follows [3]:

$$\mathcal{L}\left[{}^{\mathcal{ABC}}D_{\mathfrak{t}}^{\mathscr{D}}(\mathscr{N}(\mathfrak{t}))\right] = (s^{\mathscr{D}}(1-\mathscr{D})+\mathscr{D})^{-1}[\phi(\mathscr{D})s^{\mathscr{D}}\mathcal{L}[\mathscr{N}(\mathfrak{t})] - \phi(\mathscr{D})s^{\mathscr{D}-1}\mathscr{N}(0)]. \tag{2.3}$$

3. Formulation of Model

Assuming lifelong immunity following vaccination and that infected individuals initially transition into a less infectious inactive phase [1, 4, 23], our focus is exclusively on addressing the model, excluding asymptomatic cases. The epidemiological model is defined as $A(\mathfrak{t}) = \{\mathcal{S}(\mathfrak{t}), \mathcal{E}(\mathfrak{t}), \mathcal{I}(\mathfrak{t}), \mathcal{R}(\mathfrak{t})\}$, where $\mathcal{S}(\mathfrak{t}), \mathcal{E}(\mathfrak{t}), \mathcal{I}(\mathfrak{t})$ and $\mathcal{R}(\mathfrak{t})$ are susceptible, exposed, infected and recovered respectively. The model is detailed below:

$$\begin{cases} \dot{\mathcal{S}}(\mathfrak{t}) = -\mathcal{S}(\mathfrak{t})[\varsigma\xi\mathcal{E}(\mathfrak{t}) + (1-d)\mathcal{I}(\mathfrak{t})\varsigma - (n_1+\sigma)] + \Pi, \\ \dot{\mathcal{E}}(\mathfrak{t}) = [\varsigma\xi\mathcal{S}(\mathfrak{t}) - (\sigma+q_1+n_2)]\mathcal{E}(\mathfrak{t}) + \mathcal{S}(\mathfrak{t})\mathcal{I}(\mathfrak{t})(1-d)\varsigma, \\ \dot{\mathcal{I}}(\mathfrak{t}) = -(\sigma+\Theta+q_2)\mathcal{I}(\mathfrak{t}) + q_1\mathcal{E}(\mathfrak{t}), \\ \dot{\mathcal{R}}(\mathfrak{t}) = -\sigma\mathcal{R}(\mathfrak{t}) + n_1 S(\mathfrak{t}) + n_2\mathcal{E}(\mathfrak{t}) + q_2\mathcal{I}(\mathfrak{t}). \end{cases} \tag{3.1}$$

4. $\mathcal{ABC}$ derivative for SEIR model

This segment is used to transform the non-linear mathematical model (3.1) into an ABC fractional derivative model. This involves employing the Atangana–Baleanu fractional operator in the Caputo sense to examine the fractional dynamics of model (3.1):

$$\begin{cases} {}^{\mathcal{ABC}}D_{\mathfrak{t}}^{\eta}\mathcal{S}(\mathfrak{t}) = -\mathcal{S}(\mathfrak{t})[\varsigma\xi\mathcal{E}(\mathfrak{t}) + (1-d)\mathcal{I}(\mathfrak{t})\varsigma - (n_1+\sigma)] + \Pi, \\ {}^{\mathcal{ABC}}D_{\mathfrak{t}}^{\eta}\mathcal{E}(\mathfrak{t}) = [\varsigma\xi\mathcal{S}(\mathfrak{t}) - (\sigma+q_1+n_2)]\mathcal{E}(\mathfrak{t}) + \mathcal{S}(\mathfrak{t})\mathcal{I}(\mathfrak{t})(1-d)\varsigma, \\ {}^{\mathcal{ABC}}D_{\mathfrak{t}}^{\eta}\mathcal{I}(\mathfrak{t}) = -(\sigma+\Theta+q_2)\mathcal{I}(\mathfrak{t}) + q_1\mathcal{E}(\mathfrak{t}), \\ {}^{\mathcal{ABC}}D_{\mathfrak{t}}^{\eta}\mathcal{R}(\mathfrak{t}) = -\sigma\mathcal{R}(\mathfrak{t}) + n_1 S(\mathfrak{t}) + n_2\mathcal{E}(\mathfrak{t}) + q_2\mathcal{I}(\mathfrak{t}). \end{cases} \tag{4.1}$$

To begin with, in order to validate the biological relevance of model (4.1), we will first verify the existence and uniqueness of the solution. Additionally, we will explore the positively invariant region and ensure that the solution remains non-negative within $\mathbb{R}_+^4$

$$\zeta := \{(\mathcal{S}, \mathcal{E}, \mathcal{I}, \mathcal{R}) \in \mathbb{R}_+^4 | \mathcal{S}, \mathcal{E}, \mathcal{I}, \mathcal{R} \geq 0\}. \tag{4.2}$$

We will utilize this condition in the following three sections.

TABLE 1. Explanation of the parameters specified in model (3.1).

Parameters	Overview
$\mathcal{S}(0)$	Total susceptible persons at initial point
$\mathcal{E}(0)$	Total exposed persons at initial point
$\mathcal{I}(0)$	Total infection persons at initial point
$\mathcal{R}(0)$	Total recovered persons at initial point
Π	Population growth rate
σ	Pace of mortality due to natural causes
Θ	Coefficient for disease-induced mortality
n_1	Vaccination pace for susceptible persons
n_2	Pace of vaccination for exposed persons
ς	The average rate of contact during infection
ξ	Factor reducing the rate of inactive infection
d	Decrease in infectivity due to quarantine, isolation, and other interventions
$\xi\mathcal{E}(\mathfrak{t}) + (1-d)\mathcal{I}(\mathfrak{t})$	Count of currently infectious individuals
q_1	Transition pace from the inactive state to the infectious state
q_2	Transition pace from the infectious state to the recovered state

5. Nonlinear fractional DEs including Mittag-Leffler (M-L) non-singular kernels

Let's examine a fractional initial-value problem (IVP) described as follows [6]:

$$\begin{cases} {}^{\mathcal{ABC}}D_{\mathfrak{t}}^{\eta}u(\mathfrak{t}) = V(\mathfrak{t}, u(\mathfrak{t})), & 0 < \mathfrak{t} < \infty, \quad 0 < \mathfrak{T} < \infty, \mathfrak{t} < \mathfrak{T}, \\ u(0) = u_0. \end{cases} \tag{5.1}$$

Given $0 < \eta < 1$, and ${}^{\mathcal{ABC}}D_{\mathfrak{t}}^{\eta}u(\mathfrak{t})$ represents the Atangana-Baleanu-Caputo fractional derivative of $u(\mathfrak{t})$ represented in Equation (2.2). Next, we will formulate the existence and uniqueness of solutions for the new fractional differential equation.

5.1. **Existence and Uniqueness.** In this section, we will explore the "existence and uniqueness of the model" defined by system (4.1). The theorem outlined below will play a crucial role in this analysis.

Theorem 5.1. *A distinctive solution for a time-fractional differential equation over $\mathbb{R}_+^4$ is attainable by using the inverse Laplace transform and the convolution theorem [27],i.e.*

$$ {}^{\mathcal{ABC}}D_{\mathfrak{t}}^{\eta}\omega(\mathfrak{t}) = \delta(\mathfrak{t}), \tag{5.2}$$

is stated as

$$\omega(\mathfrak{t}) = (\phi(\eta))^{-1}\left[(1-\eta)\delta(\mathfrak{t}) + \eta(\Gamma(\eta))^{-1}\int_0^t \delta(l)(\mathfrak{t}-l)^{\eta-1}dl\right]. \tag{5.3}$$

Subsequently, we utilize Theorem 5.1 to derive the Volterra-type integral equation corresponding to (4.1):

$$\begin{cases} -\mathcal{S}(0) + \mathcal{S}(\mathfrak{t}) = \frac{1}{\phi(\eta)}(1-\eta)(F_1(\mathfrak{t},\mathcal{S})) + \eta\left[\frac{1}{\Gamma(\eta)\phi(\eta)}\right]\int_0^{\mathfrak{t}} F_1(l,\mathcal{S})(t-l)^{\eta-1}\,dl, \\[2mm] -\mathcal{E}(0) + \mathcal{E}(\mathfrak{t}) = \frac{1}{\phi(\eta)}(1-\eta)(F_2(\mathfrak{t},\mathcal{E})) + \eta\left[\frac{1}{\Gamma(\eta)\phi(\eta)}\right]\int_0^{\mathfrak{t}} F_2(l,\mathcal{E})(t-l)^{\eta-1}\,dl, \\[2mm] -\mathcal{I}(0) + \mathcal{I}(\mathfrak{t}) = \frac{1}{\phi(\eta)}(1-\eta)(F_3(\mathfrak{t},\mathcal{I})) + \eta\left[\frac{1}{\Gamma(\eta)\phi(\eta)}\right]\int_0^{\mathfrak{t}} F_3(l,\mathcal{I})(t-l)^{\eta-1}\,dl, \\[2mm] -\mathcal{R}(0) + \mathcal{R}(\mathfrak{t}) = \frac{1}{\phi(\eta)}(1-\eta)(F_4(\mathfrak{t},\mathcal{R})) + \eta\left[\frac{1}{\Gamma(\eta)\phi(\eta)}\right]\int_0^{\mathfrak{t}} F_4(l,\mathcal{R})(t-l)^{\eta-1}\,dl, \end{cases} \tag{5.4}$$

where

$$
\begin{aligned}
F_1(\mathfrak{t},\mathcal{S}) &= -\,\mathcal{S}(\mathfrak{t})[\varsigma\xi\mathcal{E}(\mathfrak{t}) + (1-d)\mathcal{I}(\mathfrak{t})\varsigma - (n_1+\sigma)] + \Pi, \\
F_2(\mathfrak{t},\mathcal{E}) &= [\varsigma\xi\mathcal{S}(\mathfrak{t}) - (\sigma+q_1+n_2)]\mathcal{E}(\mathfrak{t}) + \mathcal{S}(\mathfrak{t})\mathcal{I}(\mathfrak{t})(1-d)\varsigma, \\
F_3(\mathfrak{t},\mathcal{I}) &= -\,(\sigma+\Theta+q_2)\mathcal{I}(\mathfrak{t}) + q_1\mathcal{E}(\mathfrak{t}), \\
F_4(\mathfrak{t},\mathcal{R}) &= -\,\sigma\mathcal{R}(\mathfrak{t}) + n_1 S(\mathfrak{t}) + n_2\mathcal{E}(\mathfrak{t}) + q_2\mathcal{I}(\mathfrak{t}).
\end{aligned}
\tag{5.5}
$$

We will demonstrate that the kernels $F_c, c = 1,2,3,4$ meet the Lipschitz condition. Let $S, \mathcal{S}, E, \mathcal{E}, I, \mathcal{I},$ and $R, \mathcal{R}$ be bounded functions in a manner such that

$$
max\{\mathcal{S}, \mathcal{S}, \mathcal{E}, \mathcal{E}, I, \mathcal{I}, \mathcal{R}, \mathcal{R}\} < \Delta.
$$

For $F_1(\mathfrak{t},\mathcal{S})$ and $F_1(\mathfrak{t},\mathcal{S})$, the following inequality is satisfied:

$$
\begin{aligned}
||F_1(\mathfrak{t},\mathcal{S}) - F_1(\mathfrak{t},\mathcal{S})|| &= || -\varsigma(\xi\mathcal{E} + (1-d)\mathcal{I})(\mathcal{S}-\mathcal{S}) - (\sigma+n_1)(\mathcal{S}-\mathcal{S})|| \\
&\leq || -\varsigma(\xi\mathcal{E} + (1-d)(\mathcal{S}-\mathcal{S}))|| + || -(\sigma+n_1)(\mathcal{S}-\mathcal{S})|| \\
&= \varsigma(\xi||\mathcal{E}||_\infty + (1-d)||\mathcal{I}||_\infty)||\mathcal{S}-\mathcal{S}|| \\
&= \Delta_1||\mathcal{S}-\mathcal{S}||,
\end{aligned}
\tag{5.6}
$$

where $\Delta_1 = \varsigma(\xi||\mathcal{E}||_\infty + (1-d)||\mathcal{I}||_\infty)$, $||\mathcal{E}||_\infty = \sup|\mathcal{E}|$, and $||\mathcal{I}||_\infty = \sup|\mathcal{I}|$. Therefore, we will demonstrate that $F_1(\mathfrak{t},\mathcal{S})$ meets the Lipschitz condition as stated in Theorem 5.1. The general Lipschitz condition is described in Assumption 1 of [7]. Using a similar approach, we will examine the following inequalities to establish this:

$$
\begin{aligned}
||F_2(\mathfrak{t},\mathcal{E}) - F_2(\mathfrak{t},\mathcal{E})|| &\leq \Delta_2||\mathcal{E}-\mathcal{E}||, \\
||F_3(\mathfrak{t},\mathcal{I}) - F_3(\mathfrak{t},\mathcal{I})|| &= \Delta_3||\mathcal{I}-\mathcal{I}||, \\
||F_4(\mathfrak{t},\mathcal{R}) - F_4(\mathfrak{t},\mathcal{R})|| &= \Delta_4||\mathcal{R}-\mathcal{R}||.
\end{aligned}
\tag{5.7}
$$

Here $\Delta_2 = ||\mathcal{S}||_\infty\varsigma\xi + \sigma + q_1 + n_2$, $\Delta_3 = \sigma + \gamma + q_2$, and $\Delta_4 = \sigma$. Therefore, the Lipschitz condition is also fulfilled by the kernel F_c for $c = 2,3,4$. In addition, F_c for $c = 2,3,4$ are reduced if $0 \leq \Delta_c < 1$, $c = 2,3,4$. Additionally, the existence of a solution to (4.1) is examined using the fixed-point theorem. The recursive form of (5.4) is represented by the following formulas:

$$
\begin{aligned}
\mathcal{S}_p(\mathfrak{t}) &= \frac{1}{\phi(\eta)}(1-\eta)(F_1(\mathfrak{t},\mathcal{S}_{p-1})) + \eta\left[\frac{1}{\phi(\eta)\Gamma(\eta)}\right]\int_0^\mathfrak{t}(\mathfrak{t}-l)^{\eta-1}F_1(l,\mathcal{S}_{p-1})dl, \\
\mathcal{E}_p(\mathfrak{t}) &= \frac{1}{\phi(\eta)}(1-\eta)(F_2(\mathfrak{t},\mathcal{E}_{p-1})) + \eta\left[\frac{1}{\phi(\eta)\Gamma(\eta)}\right]\int_0^\mathfrak{t}(\mathfrak{t}-l)^{\eta-1}F_2(l,\mathcal{E}_{p-1})dl, \\
\mathcal{I}_p(\mathfrak{t}) &= \frac{1}{\phi(\eta)}(1-\eta)(F_3(\mathfrak{t},\mathcal{I}_{p-1})) + \eta\left[\frac{1}{\phi(\eta)\Gamma(\eta)}\right]\int_0^\mathfrak{t}(\mathfrak{t}-l)^{\eta-1}F_3(l,\mathcal{I}_{p-1})dl, \\
\mathcal{R}_p(\mathfrak{t}) &= \frac{1}{\phi(\eta)}(1-\eta)(F_4(\mathfrak{t},\mathcal{R}_{p-1})) + \eta\left[\frac{1}{\phi(\eta)\Gamma(\eta)}\right]\int_0^\mathfrak{t}(\mathfrak{t}-l)^{\eta-1}F_4(l,\mathcal{R}_{p-1})dl,
\end{aligned}
\tag{5.8}
$$

The initial conditions for (5.8) are given by $\mathcal{S}_0(\mathfrak{t}) = \mathcal{S}(0)$, $\mathcal{E}_0(\mathfrak{t}) = \mathcal{E}(0)$, $\mathcal{I}_0(\mathfrak{t}) = \mathcal{I}(0)$, and $\mathcal{R}_0(\mathfrak{t}) = \mathcal{R}(0)$. The succeeding terms in (5.8) can be expressed as follows:

$$
\begin{aligned}
\Phi_{1,p}(\mathfrak{t}) &= -\mathcal{S}_{p-1}(\mathfrak{t}) + \mathcal{S}_p(\mathfrak{t}) = \frac{1}{\phi(\eta)}(1-\eta)\left(F_1(\mathfrak{t},\mathcal{S}_{p-1}) - F_1(\mathfrak{t},\mathcal{S}_{p-2})\right) \\
&\quad + \eta\left[\frac{1}{\phi(\eta)\Gamma(\eta)}\right]\int_0^\mathfrak{t}(\mathfrak{t}-l)^{\eta-1}(F_1(l,\mathcal{S}_{p-1}) - F_1(l,\mathcal{S}_{p-2}))dl, \\
\Phi_{2,p}(\mathfrak{t}) &= -\mathcal{E}_{p-1}(\mathfrak{t}) + \mathcal{E}_p(\mathfrak{t}) = \frac{1}{\phi(\eta)}(1-\eta)(F_2(\mathfrak{t},\mathcal{E}_{p-1}) - F_2(\mathfrak{t},\mathcal{E}_{p-2}))
\end{aligned}
$$

$$+ \eta \left[\frac{1}{\phi(\eta)\Gamma(\eta)} \right] \int_0^t (t-l)^{\eta-1} (F_2(l, \mathcal{E}_{p-1}) - F_2(l, \mathcal{E}_{p-2})) dl, \tag{5.9}$$

$$\Phi_{3,p}(t) = -\mathcal{I}_{p-1}(t) + \mathcal{I}_p(t) = \frac{1}{\phi(\eta)}(1-\eta)(F_3(t, \mathcal{I}_{p-1}) - F_3(t, \mathcal{I}_{p-2}))$$

$$+ \eta \left[\frac{1}{\phi(\eta)\Gamma(\eta)} \right] \int_0^t (t-l)^{\eta-1} (F_3(l, \mathcal{I}_{p-1}) - F_3(l, \mathcal{I}_{p-2})) dl,$$

$$\Phi_{4,p}(t) = -\mathcal{R}_{p-1}(t) + \mathcal{R}_p(t) = \frac{1}{\phi(\eta)}(1-\eta)(F_4(t, \mathcal{R}_{p-1}) - F_4(t, \mathcal{R}_{p-2}))$$

$$+ \eta \left[\frac{1}{\phi(\eta)\Gamma(\eta)} \right] \int_0^t (t-l)^{\eta-1} (F_4(l, \mathcal{R}_{p-1}) - F_4(l, \mathcal{R}_{p-2})) dl,$$

and thus, we have

$$\mathcal{S}_p(t) = \sum_{i=1}^p \Phi_{1,c}(t), \qquad\qquad \mathcal{E}_p(t) = \sum_{c=1}^p \Phi_{2,c}(t),$$

$$\mathcal{I}_p(t) = \sum_{c=1}^p \Phi_{3,c}(t), \qquad\qquad \mathcal{R}_p(t) = \sum_{c=1}^p \Phi_{4,c}(t). \tag{5.10}$$

To find the norm of both sides of (5.9), we employ (5.6) and (5.7), yielding the following results:

$$||\Phi_{1,p}(t)|| \leq (1-\eta)\frac{1}{\phi(\eta)}\Delta_1 ||\Phi_{1,p-1}|| + \eta \left[\frac{1}{\phi(\eta)\Gamma(\eta)} \right] \Delta_1 \int_0^t ||\Phi_{1,p-1}(l)|| (t-l)^{\eta-1} dl,$$

$$||\Phi_{2,p}(t)|| \leq (1-\eta)\frac{1}{\phi(\eta)}\Delta_2 ||\Phi_{2,p-1}|| + \eta \left[\frac{1}{\phi(\eta)\Gamma(\eta)} \right] \Delta_2 \int_0^t ||\Phi_{2,p-1}(l)|| (t-l)^{\eta-1} dl,$$

$$||\Phi_{3,p}(t)|| \leq (1-\eta)\frac{1}{\phi(\eta)}\Delta_3 ||\Phi_{3,p-1}|| + \eta \left[\frac{1}{\phi(\eta)\Gamma(\eta)} \right] \Delta_3 \int_0^t ||\Phi_{3,p-1}(l)|| (t-l)^{\eta-1} dl,$$

$$||\Phi_{4,p}(t)|| \leq (1-\eta)\frac{1}{\phi(\eta)}\Delta_4 ||\Phi_{4,p-1}|| + \eta \left[\frac{1}{\phi(\eta)\Gamma(\eta)} \right] \Delta_4 \int_0^t ||\Phi_{4,p-1}(l)|| (t-l)^{\eta-1} dl.$$

Next, we will introduce the following theorem:

Theorem 5.2. *Model* (4.1) *possesses a sole outcome if there exists a* t_{max} *such that*

$$(1-\eta)\frac{\Delta_1}{\phi(\eta)} + t_{max}^\eta \frac{\Delta_c}{\phi(\eta)\Gamma(\eta)} < 1, \qquad c = 1, 2, 3, 4. \tag{5.11}$$

Proof. Assume that $\mathcal{S}(t)$, $\mathcal{E}(t)$, $\mathcal{I}(t)$, and $\mathcal{R}(t)$ are bounded functions. From the previous proof, these functions meet the Lipschitz condition. Given (5.11) and using the principle of successive approximations, the following inequalities hold:

$$|\Phi_{1,p}(t)|| \leq ||\mathcal{S}_0|| \left(\frac{(1-\eta)\Delta_1}{\phi(a)} + \frac{t^\eta \Delta_1}{\phi(\eta)\Gamma(\eta)} \right)^p,$$

$$||\Phi_{2,p}(t)|| \leq ||\mathcal{E}_0|| \left(\frac{(1-\eta)\Delta_2}{\phi(\eta)} + \frac{t^\eta \Delta_2}{\phi(\eta)\Gamma(\eta)} \right)^p,$$

$$||\Phi_{3,p}(t)|| \leq ||\mathcal{I}_0|| \left(\frac{(1-\eta)\Delta_3}{\phi(\eta)} + \frac{t^\eta \Delta_3}{\phi(\eta)\Gamma(\eta)} \right)^p, \tag{5.12}$$

$$||\Phi_{4,p}(t)|| \leq ||\mathcal{R}_0|| \left(\frac{(1-\eta)\Delta_4}{\phi(\eta)} + \frac{t^\eta \Delta_4}{\phi(\eta)\Gamma(\eta)} \right)^p.$$

To establish that (5.4) represents the solution of (4.1), we have demonstrated the existence and smoothness of (5.10) by ensuring that $|\Phi_{i,p}(t)|$ approaches to zero for $c = 1, 2, \ldots, 7$ as $t \to t_{max}$. Let us proceed with the assumption that

$$
\begin{aligned}
-\mathcal{S}(0) + \mathcal{S}(t) &= -Y_{1,p}(t) + \mathcal{S}_p(t), \\
-\mathcal{E}(0) + \mathcal{E}(t) &= -Y_{2,p}(t) + \mathcal{E}_p(t), \\
-\mathcal{I}(0) + \mathcal{I}(t) &= -Y_{3,p}(t) + \mathcal{I}_p(t), \\
-\mathcal{R}(0) + \mathcal{R}(t) &= -Y_{4,p}(t) + \mathcal{I}_p(t).
\end{aligned}
\tag{5.13}
$$

In this context, $Y_{c,p}(t)$ for $c = 1, 2, 3, 4$ denotes the residual expressions of the series solutions. Each residual expression $Y_{c,p}(t)$ is associated with a norm defined as:

$$
\begin{aligned}
||Y_{1,n}(t)|| &\leq \frac{1-\eta}{\phi(\eta)} ||F_1(t, \mathcal{S}) - F_1(t, \mathcal{S}_{p-1})|| + \left[\frac{1}{\phi(\eta)\Gamma(\eta)} \right] \eta \int_0^t ||F_1(l, \mathcal{S}) - F_1(l, S_{n-1})|| (t-l)^{\eta-1} dl \\
&\leq ||\mathcal{S} - \mathcal{S}_{n-1}|| \left(1 - \eta + \frac{t^\eta}{\Gamma(\eta)} \right) \frac{\Delta_1}{\phi(\eta)}.
\end{aligned}
\tag{5.14}
$$

By applying an iterative approach to inequality (5.14), at $t = t_{\max}$, we achieve

$$
||Y_{1,n}(t)|| \leq \left(1 - \eta + \frac{t_{max}^\eta}{\Gamma(\eta)} \right) \frac{\Delta_1^{n+1} M}{\phi(\eta)}.
\tag{5.15}
$$

We establish that $||Y_{1,n}(t)||$ tends to zero as n approches to ∞. By employing a nearly identical method, we also find that $||Y_{i,n}(t)||$ tends to 0 for $i = 2, 3, 4$. Therefore, functions that satisfy (5.4) are solutions to (4.1), confirming the uniqueness of the solution for model (4.1). Let $S(t), E(t), I(t)$ and $R(t)$ represent another set of solutions for model (4.1). Then, the following equation holds:

$$
-\mathcal{S}^*(t) + \mathcal{S}(t) = \frac{1-\eta}{\phi(\eta)} (-F_1(t, \mathcal{S}^*) + F_1(t, \mathcal{S}) + \frac{\eta}{\phi(\eta)\Gamma(\eta)} \int_0^t (t-l)^{\eta-1} (-F_1(t, \mathcal{S}^*) + F_1(t, \mathcal{S}) dl.
\tag{5.16}
$$

Applying the $||.||$ to both sides of (5.16) using the same method as in (5.10) and (5.12), we obtain

$$
\left(1 - \frac{(1-\eta)\Delta_1}{\phi(\eta)} - \frac{t^\eta \Delta_1}{\phi(\eta)\Gamma(\eta)} \right) || - \mathcal{S}^*(t) + \mathcal{S}(t)|| \leq 0.
\tag{5.17}
$$

We confirm that for $t = t_{max}$, we have

$$
\left(1 - \frac{(1-\eta)\Delta_1}{\phi(\eta)} - \frac{t^\eta \Delta_1}{\phi(\eta)\Gamma(\eta)} \right) \geq 0.
$$

According to this theorem, $|| - \mathcal{S}^*(t) + \mathcal{S}(t)|| = 0$, which gives that $\mathcal{S}(t) = \mathcal{S}^*(t)$. Similarly, by following this procedure, which gives us $\mathcal{E}(t) = \mathcal{E}^*(t)$, $\mathcal{I}(t) = \mathcal{I}^*(t)$, and $\mathcal{R}(t) = \mathcal{R}^*(t)$. This concludes the proof of the existence and uniqueness of the solution (4.1). □

6. Region of positivity invariance

In this section, our goal is to examine the boundary values of solutions $A = (\mathcal{S}, \mathcal{E}, \mathcal{I}, \mathcal{R})$ for the set of equations in (4.1) under non-decreasing preliminary conditions. We will show the existence of a positively invariant feasible region in $\mathbb{R}_+^4$ concerning model (4.1). To achieve this, we introduce the subsequent theorem:

Theorem 6.1. *Let us assume that*

$$
\mathcal{F}(t) = \mathcal{E}(t) + \mathcal{I}(t) + \mathcal{R}(t) + \mathcal{S}(t),
$$

$$
\zeta = \left\{ A(t) \in \mathbb{R}_+^4 : 0 < \mathcal{N} \leq \frac{\Pi}{\sigma + n_1} \right\}.
$$

Then the set ζ is a closed and positively invariant set for (4.1).

Proof. We have verified that $\mathcal{F}(\mathfrak{t})$ represents the total population. Computing fractional derivative in ABC sense at $\eta \in (0,1]$, we acquire:

$$^{ABC}D_{\mathfrak{t}}^{\eta}\mathcal{F}(\mathfrak{t}) = \Pi - \sigma\mathcal{F}(\mathfrak{t}) - \Theta\mathcal{I}(\mathfrak{t}). \tag{6.1}$$

Implementing Laplace transform [8] to mathematical expression (6.1), the following outcomes are derived:

$$\mathcal{L}[\,^{ABC}D_{\mathfrak{t}}^{\eta}(\mathcal{F}(\mathfrak{t}))] = \mathcal{L}[\Pi - \sigma\mathcal{F}(\mathfrak{t}) - \Theta\mathcal{I}(\mathfrak{t})]$$
$$\leq \mathcal{L}[\Pi - \sigma\mathcal{F}(\mathfrak{t})],$$

$$\frac{\phi(\eta)s^{\eta}\mathcal{F}(s)}{s^{\eta}(1-\eta)+\eta} + \sigma\mathcal{F}(s) \leq \frac{\Pi}{s} + \frac{\phi(\eta)s^{\eta-1}\mathcal{F}(0)}{s^{\eta}(1-\eta)+\eta}. \tag{6.2}$$

Rewriting (6.2) about $\mathcal{F}(s)$, which is the Laplace transform of $\{\mathcal{F}(\mathfrak{t})(s)\}$ and where $\mathcal{F}(0)$ denotes preliminary condition, leads us to the following expression:

$$\mathcal{F}(s) \leq \frac{\Pi s^{-1}[s^{\eta}-\eta(s^{\eta}-1)] + \phi(\eta)s^{\eta-1}\mathcal{F}(0)}{\sigma[s^{\eta}-\eta(s^{\eta}-1)] + s^{\eta}\phi(\eta)}.$$

Therefore,

$$\mathcal{F}(s) \leq \frac{\Pi s^{-1}[s^{\eta}-\eta(s^{\eta}-1)]}{[\phi(\eta)+\sqcap-\eta\sigma]s^{\eta}+\eta\sigma} + \frac{\phi(\eta)s^{\eta-1}\mathcal{F}(0)}{[\phi(\eta)+\sqcap-\eta\sigma]s^{\eta}+\eta\sigma}$$

$$= \left(\frac{-\eta\Pi+\Pi+\phi(\eta)\mathcal{F}(0)}{\phi(\eta)-\eta\sigma+\sigma}\right)\left[\frac{s^{\eta-1}}{s^{\eta}+\frac{\eta\sigma}{\phi(\eta)-\eta\sigma+\sigma}}\right] + \left(\frac{\eta\Pi}{\phi(\eta)-\eta\sigma+\sigma}\right)\left[\frac{s^{\eta-(\eta+1)}}{s^{\eta}+\frac{\eta\sigma}{\phi(\eta)-\eta\sigma+\sigma}}\right].$$

Employ the $\mathcal{L}^{-1}$ to each side of the above equation, We derive the subsequent set of inequalities:

$$\mathcal{F}(s) \leq \left(\frac{\Pi-\eta\Pi+\phi(\eta)\mathcal{F}(0)}{\phi(\eta)+\sigma-\eta\sigma}\right)E_{\eta,1}\left(\frac{-\eta\sigma t^{\eta}}{\phi(\eta)+\sigma-\eta\sigma}\right) + \left(\frac{\eta\Pi}{\phi(\eta)+\sigma-\eta\sigma}\right)E_{\eta,\eta+1}\left(\frac{-\eta\sigma t^{\eta}}{\phi(\eta)+\sigma-\eta\sigma}\right). \tag{6.3}$$

The Mittag-Leffler function with two variables, where $\mathcal{G} > 0$ and $\mathcal{H} > 0$, is characterized by the following definition:

$$E_{\mathcal{G},\mathcal{H}}(Y) = \sum_{j=0}^{\infty}\frac{Y^{j}}{\mathcal{G}j+\mathcal{H}}.$$

Laplace transform of this function is

$$\mathcal{L}[t^{\mathcal{H}-1}E_{\mathcal{G},\mathcal{F}}(\pm\nu t^{\mathcal{G}})] = \frac{s^{\mathcal{G}-\mathcal{H}}}{s^{\eta}\mp\nu}.$$

Given that $s > |\nu|^{\frac{1}{\mathcal{G}}}$. Mittag-Leffler function is described by [11] as follows:

$$E_{\mathcal{G},\mathcal{H}}(Y) = \frac{1}{Y}\left[\frac{E_{\mathcal{G},\mathcal{H}-\mathcal{G}}(Y)\Gamma(\mathcal{H}-\mathcal{G})-1}{\Gamma(\mathcal{H}-\mathcal{G})}\right]. \tag{6.4}$$

The publication [16] outlines the asymptotic characteristics of the Mittag-Leffler function as follows:

$$E_{\mathcal{H},\mathcal{H}+1}(Y) \approx \sum_{j=1}^{i}\frac{Y^{-j}}{\mathcal{H}+(\mathcal{H}+1)j} + \mathcal{O}(|Y|^{-1-i}), |Y| \to \infty, \frac{\mathcal{H}\pi}{2} < |argY| \leq \pi. \tag{6.5}$$

Referring to Equations (6.3) and (6.4), and considering the convergence behavior outlined by the Mittag-Leffler equation (6.5), as $\mathfrak{t}$ approaches infinity, it becomes apparent that $\mathcal{N}(\mathfrak{t})$ is bounded above by $\frac{\Pi}{x}$. Consequently, the set ζ can be regarded as positively invariant within the context of system (4.1). $\square$

6.1. **Stability characteristics of stable points.** Here, we are going to examine the local stability of the stable points, referencing appropriate sources [15, 20, 24] for stability analysis. To evaluate the stability characteristics of the stable points, we first need to identify these stable points. The model (4.1) presents two stable points: the infection-free stable point (IFSP) and the endemic stable point (ESP).

6.2. **Infection-free stable point.** Setting the R.H.S. of the mathematical expressions given in (4.1) equal to zero, we obtain the infection-free stable point (D_f), written as follows:

$$D_f = (\mathcal{S}_f, \mathcal{E}_f, \mathcal{I}_f, \mathcal{R}_f) = \left(\frac{\Pi}{x}, 0, 0, \frac{\Pi}{\sigma x} \right),$$

where $x = \sigma + n_1$. By applying the next-generation matrix method [12], we calculated the basic reproductive number B_r for the system defined by the equations in (4.1) as follows:

$$\mathscr{F}_{D_f} = \begin{bmatrix} -[\varsigma \xi \mathcal{E} + (1-d)\varsigma \mathcal{I}] & -\varsigma \mathcal{S} \mathcal{E} & -\varsigma \mathcal{S} + \varsigma \mathcal{S} d \\ \varsigma \xi \mathcal{E} + (1-d)\mathcal{I}\varsigma & \varsigma \mathcal{S} \mathcal{E} & \varsigma \mathcal{S}(1-d) \\ 0 & 0 & 0 \end{bmatrix},$$

$$\mathscr{V}_{D_f} = \begin{bmatrix} \sigma + n_1 & 0 & 0 \\ 0 & \sigma + q_1 + n_2 & 0 \\ 0 & -q_1 & \sigma + \Theta + q_2 \end{bmatrix}, \tag{6.6}$$

$$\mathscr{V}_{D_f}^{-1} = \begin{bmatrix} \frac{1}{\sigma + n_1} & 0 & 0 \\ 0 & \frac{1}{\sigma + q_1 + n_2} & 0 \\ 0 & \frac{q_1}{(\sigma + q_1 + n_2)(\sigma + \Theta + q_2)} & \frac{1}{\sigma + \Theta + q_2} \end{bmatrix},$$

B_r is stated as the maximum eigenvalue of the matrix $(\mathscr{F}_{D_f} V_{D_f}^{-1})$ and is obtained when

$$B_r = \frac{\varsigma \Pi(\xi y + q_1(1-d))}{xyz},$$

where

$$x = \sigma + n_1, \quad y = \sigma + \Theta + q_2, \quad z = \sigma + q_1 + n_2.$$

Lemma 6.2. *The infection-free stable point (D_f) exhibits local stability when $R_0 < 1$; otherwise, D_f is unstable.*

Proof. Configuring the L.H.S. of the mathematical expression in system (4.1) as

$$a' = -\mathcal{S}(\mathfrak{t})[\varsigma \xi \mathcal{E}(\mathfrak{t}) + (1-d)\mathcal{I}(\mathfrak{t})\varsigma - (n_1 + \sigma)] + \Pi,$$
$$b' = [\varsigma \xi \mathcal{S}(\mathfrak{t}) - (\sigma + q_1 + n_2)]\mathcal{E}(\mathfrak{t}) + \mathcal{S}(\mathfrak{t})\mathcal{I}(\mathfrak{t})(1-d)\varsigma,$$
$$c' = -(\sigma + \Theta + q_2)\mathcal{I}(\mathfrak{t}) + q_1 \mathcal{E}(\mathfrak{t}).$$

The Jacobian matrix evaluated at D_f is expressed as

$$J_{D_f} = \begin{bmatrix} -(\sigma + n_1) & -\frac{\Pi \varsigma \xi}{\sigma + n_1} & -\frac{\Pi \varsigma (1-d)}{\sigma + n_1} \\ 0 & \frac{\Pi \varsigma \xi}{\sigma + n_1} - (\sigma + q_1 + n_2) & \frac{\Pi \varsigma (1-d)}{\sigma + n_1} \\ 0 & q_1 & -(\sigma + \Theta + q_2) \end{bmatrix},$$

or

$$J_{D_f} = \begin{bmatrix} -x & -\frac{\Pi \varsigma \xi}{x} & -\frac{\Pi \varsigma (1-d)}{x} \\ 0 & \frac{\Pi \varsigma \xi}{x} - z & \frac{\Pi \varsigma (1-d)}{x} \\ 0 & q_1 & -y \end{bmatrix}.$$

Let $x = \sigma + n_1, y = \sigma + \Theta + q_2$, and $z = \sigma + q_1 + n_2$. To find the eigenvalues, we solve $\det(\lambda I - J_{D_f}) = 0$. It is evident that $\lambda_1 = -x < 0$. The remaining two eigenvalues of the system can be determined by solving $\det(\lambda I - J_{D_f}^*)$, as detailed below:

$$\det(\lambda - J_{D_f}^*) = \det \begin{bmatrix} \lambda - \left(\frac{\Pi \varsigma \xi}{x} - z \right) & -\frac{\Pi \varsigma (1-d)}{x} \\ -q_1 & \lambda + y \end{bmatrix}.$$

The characteristic equation for $J_{D_f}^*$ can be expressed as:

$$\lambda^2 + \mathcal{K}_1 \lambda + \mathcal{K}_0 = 0,$$

where

$$\mathcal{K}_1 = y + z - \frac{\Pi\varsigma\xi}{x},$$

$$\mathcal{K}_0 = yz + \frac{\Pi\varsigma q_1 d}{x} - \frac{\Pi\varsigma}{x}(q_1 + \xi y).$$

Based on the Routh-Hurwitz criteria (R-H.C) , if $\mathcal{K}_1 > 0$ and $\mathcal{K}_0 > 0$, then all eigenvalues will possess negative real parts. Consequently, with $\mathcal{K}_1 > 0$ and $\mathcal{K}_0 > 0$, we can ascertain that the infection-free stable point is locally asymptotically stable when $B_r < 1$, and not stable when $B_r > 1$. This finding concludes the proof. $\qquad\square$

6.3. **Endemic stable point.** If $B_r > 1$, then there will be found an endemic stable point D_p such as $D_p = (\mathcal{S}_p, \mathcal{E}_p, \mathcal{I}_p, \mathcal{R}_p)$, where

$$\mathcal{S}_p = \frac{\Pi}{xB_r},$$

$$\mathcal{E}_p = \frac{\Pi}{z}\left(1 - \frac{1}{B_r}\right),$$

$$\mathcal{I}_p = \frac{\Pi q_1}{yz}\left(1 - \frac{1}{B_r}\right),$$

$$\mathcal{R}_p = \frac{\Pi}{\sigma}\left[\frac{n_1}{xB_r} + \frac{1}{z}\left(n_2 + \frac{q_1}{y}\right)\left(1 - \frac{1}{B_r}\right)\right].$$

Lemma 6.3. *The system represented by D_p reveals local asymptotic stability whether $B_r > 1$ and not stable if $B_r < 1$.*

Proof. The Jacobian matrix computed at D_p is formulated as:

$$J_{D_p} = \begin{bmatrix} -\frac{xyzB_r}{\Pi} - x & -\frac{\Pi\varsigma\xi}{xB_r} & -\frac{(1-d)\Pi\varsigma}{xB_r} \\ \frac{xyzB_r}{\Pi} & \frac{\Pi\varsigma\xi}{xB_r} - z & \frac{(1-d)\Pi\varsigma}{xB_r} \\ 0 & q_1 & -y \end{bmatrix},$$

or

$$J_{D_p} = \begin{bmatrix} -J_1 - J_2 & -J_3 & -J_4 \\ J_1 & J_3 - J_5 & J_4 \\ 0 & J_6 & -J_7 \end{bmatrix},$$

where

$$J_1 = \frac{xyzB_r}{\Pi}, \quad J_2 = x, \quad J_3 = \frac{\Pi\varsigma\xi}{xB_r}, \quad J_4 = \frac{(1-d)\Pi\varsigma}{xB_r}, \quad J_5 = z, \quad J_6 = q_1, \quad J_7 = y.$$

To determine the eigenvalues, we solve the characteristic equation $\det(J_{D_p} - \lambda I) = 0$, with J_{D_p} representing the Jacobian matrix. Hence,

$$\lambda^3 + C_2\lambda^2 + C_1\lambda + C_0 = 0,$$

where

$$C_2 = \frac{xyzB_r}{\Pi} + \frac{\Pi\varsigma\xi}{xB_r} + x + y + z,$$

$$C_1 = xy + yz + xz + \frac{xy^2zB_r}{\Pi} + \frac{xyz^2B_r}{\Pi} + \frac{\Pi^2\varsigma^2\xi d}{a^2B_r{}^2} + \frac{\Pi\varsigma z}{xB_r} + \frac{\Pi\varsigma q_1}{xB_r} - \frac{\Pi\varsigma\xi y}{xB_r} - \frac{\Pi\varsigma\xi}{B_r} - \frac{\Pi^2\varsigma^2\xi}{x^2B_r{}^2} - \frac{\Pi\varsigma dz}{xR_0} - \frac{\Pi\varsigma q_1}{xB_r},$$

$$C_0 = \frac{xy^2z^2B_r}{\Pi} + 2\varsigma q_1 dyz + xyz - \frac{\Pi\varsigma\xi y}{B_r}(y + q_1) - 2\varsigma q_1 yz.$$

Using the R-H.C, when $C_1 > 0$, $C_0 > 0$, and $C_1C_2 > C_0$, all eigenvalues exhibit negative real parts. With these conditions satisfied, if $B_r > 1$, then the endemic stable point is deemed locally asymptotically stable, while if $B_r < 1$, it is unstable. This completes the proof. $\qquad\square$

6.4. **Global stability.**

Lemma 6.4. *If $B_r \leq 1$, then the infection-free stable point D_f is globally asymptotically stable.*

Proof. Taking into account the Lyapunov function [5] defined in $\mathbb{R}_+^4$, it is expressed as follows:

$$\mathbb{L}_{D_f}(\mathcal{S}, \mathcal{E}, \mathcal{I}, \mathcal{R}) = \mathcal{S}_f \left(\frac{\mathcal{S}}{\mathcal{S}_f} - \ln\left(\frac{\mathcal{S}}{\mathcal{S}_f} \right) - 1 \right) + \mathcal{E} + \frac{z}{q_1}\mathcal{I}. \tag{6.7}$$

By implementing the ABC fractional time derivative on each side of the mathematical expression (6.7) yields

$$^{ABC}D_t^\eta(\mathbb{L}_{D_f}) = \left(1 - \frac{\mathcal{S}_f}{\mathcal{S}} \right) \, {}^{ABC}D_t^\eta(\mathcal{S}) + \, {}^{ABC}D_t^\eta(\mathcal{E}) + \frac{z}{q_1} \, {}^{ABC}D_t^\eta(\mathcal{I}).$$

Utilize (4.1), we have

$$
\begin{aligned}
^{ABC}D_t^\eta(\mathbb{L}_{D_f}) =& \Pi - x\mathcal{S} - \frac{\mathcal{S}_f}{\mathcal{S}}[\Pi - \varsigma\mathcal{S}(\xi\mathcal{E} + (1-d)\mathcal{I}) - x\mathcal{S}] - \frac{yz}{q_1}I \\
=& -x\mathcal{S} - \frac{\Pi\mathcal{S}_f}{\mathcal{S}} + \varsigma\mathcal{S}_f(\xi\mathcal{E} + (1-d)\mathcal{I}) - \frac{yz}{q_1}\mathcal{I} \\
=& -x\mathcal{S} - \frac{\Pi\mathcal{S}_f}{\mathcal{S}} + xyz\left(\frac{\mathcal{S}_f}{\mathcal{S}} \right)B_r - \frac{yz}{q_1}\mathcal{I} \\
\leq& -x\mathcal{S} - \frac{\Pi\mathcal{S}_f}{\mathcal{S}} + B_r - \frac{yz}{q_1}\mathcal{I}.
\end{aligned}
$$

It is evident that $^{ABC}D_t^\eta(\mathbb{L}_{D_f}) \leq 0$. We conclude that the infection-free stable point D_f is globally asymptotically stable. $\qquad\square$

Lemma 6.5. *If $B_r \geq 1$, then the endemic stable point D_p is globally asymptotically stable.*

Proof. Let's examine the Lyapunov function defined on $\mathbb{R}_+^4$:

$$\mathbb{L}_{D_p} = \rho_1\left(\mathcal{S} - \mathcal{S}_p - \mathcal{S}_p \ln \frac{\mathcal{S}}{\mathcal{S}_p} \right) + \rho_2\left(\mathcal{E} - \mathcal{E}_p - \mathcal{E}_p \ln \frac{\mathcal{E}}{\mathcal{E}_p} \right) + \rho_3\left(\mathcal{I} - \mathcal{I}_f - \mathcal{I}_f \ln \frac{\mathcal{I}}{\mathcal{I}_f} \right) + \rho_4\left(\mathcal{R} - \mathcal{R}_f - \mathcal{R}_f \ln \frac{\mathcal{R}}{\mathcal{R}_f} \right), \tag{6.8}$$

where

$$\rho_1 = \frac{1}{x}, \quad \rho_2 = \frac{B_r - 1}{z}, \quad \rho_3 = \frac{1}{y}, \quad \rho_4 = \frac{1}{\sigma}.$$
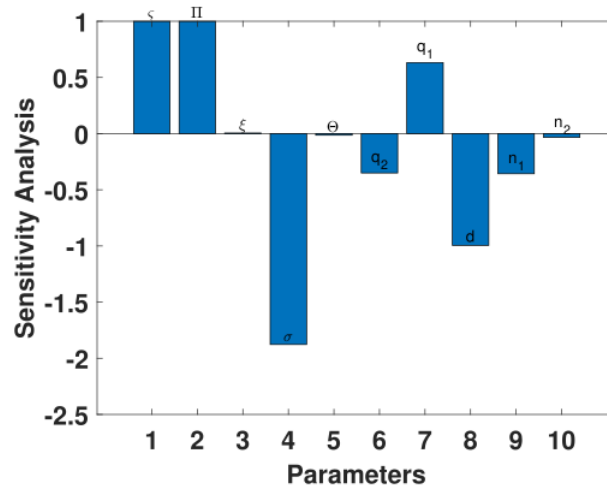
The ABC fractional time derivative of (6.8) derived as:

$$
\begin{aligned}
^{ABC}D_t^\eta(\mathbb{L}_{D_p}) =& \rho_1\left(1 - \frac{\mathcal{S}_p}{\mathcal{S}} \right) \, {}^{ABC}D_t^\eta(\mathcal{S}) + \rho_2\left(1 - \frac{\mathcal{E}_p}{\mathcal{E}} \right) \, {}^{ABC}D_t^\eta(\mathcal{E}) \\
&+ \rho_3\left(1 - \frac{\mathcal{I}_p}{\mathcal{I}} \right) \, {}^{ABC}D_t^\eta(\mathcal{I}) + \rho_4\left(1 - \frac{\mathcal{R}_p}{\mathcal{R}} \right) \, {}^{ABC}D_t^\eta(\mathcal{R}) \\
=& \rho_1\left(1 - \frac{\mathcal{S}_p}{\mathcal{S}} \right)(\Pi - \varsigma\mathcal{S}(\xi\mathcal{E} + (1-d)\mathcal{I} - x\mathcal{S})) + \rho_2\left(1 - \frac{\mathcal{E}_p}{\mathcal{E}} \right)(\varsigma\mathcal{S}(\xi\mathcal{E} + (1-d)\mathcal{I} - z\mathcal{E})) \\
&+ \rho_3\left(1 - \frac{\mathcal{I}_p}{\mathcal{I}} \right)(q_1\mathcal{E} - y\mathcal{I}) + \rho_4\left(1 - \frac{\mathcal{R}_p}{\mathcal{R}} \right)(n_1\mathcal{S} + n_2\mathcal{E} + q_2\mathcal{I} - \sigma\mathcal{R}).
\end{aligned} \tag{6.9}
$$

Exerting the endemic conditions as

$$
\begin{aligned}
&\Pi - \varsigma\mathcal{S}_p(\xi\mathcal{E}_p + (1-d)\mathcal{I}_p) = x\mathcal{S}_p, \\
&\varsigma\mathcal{S}_p(\xi\mathcal{E}_p + (1-d)\mathcal{I}_p) = z\mathcal{E}_p, \\
&q_1\mathcal{E}_p = y\mathcal{I}_p, \\
&n_1\mathcal{S}_p + n_2\mathcal{E}_p + q_2\mathcal{I}_p = \sigma\mathcal{R}_p.
\end{aligned}
$$

Therefore, (6.9) becomes

$$^{\mathcal{ABC}}D_{\mathfrak{t}}^{\eta}(\mathbb{L}_{D_p}) \leq \frac{1}{x}\left(1 - \frac{\mathcal{S}_p}{\mathcal{S}}\right)(x\mathcal{S}_p - x\mathcal{S}) + \left(\frac{B_r - 1}{z}\right)(z\mathcal{E}_p - z\mathcal{E})$$

$$+ \frac{1}{y}\left(1 - \frac{\mathcal{E}_p}{\mathcal{E}}\right)(y\mathcal{I}_p - y\mathcal{I}) + \frac{1}{\sigma}\left(1 - \frac{\mathcal{R}_p}{\mathcal{R}}\right)(\sigma\mathcal{R}_p - \sigma\mathcal{R})$$

$$= -\frac{(\mathcal{S} - \mathcal{S}_p)^2}{\mathcal{S}} - \frac{(\mathcal{E} - \mathcal{E}_p)^2}{\mathcal{E}}(B_r - 1) - \frac{(\mathcal{I} - \mathcal{I}_p)^2}{\mathcal{I}} - \frac{(\mathcal{R} - \mathcal{R}_p)^2}{\mathcal{R}}.$$

Clearly, $^{\mathcal{ABC}}D_{\mathfrak{t}}^{\eta}(\mathbb{L}_{D_p}) \leq 0$. Therefore, the endemic stable point D_p is globally asymptotically stable. □

7. Sensitivity analysis

Conducting sensitivity analysis is crucial for assessing how the variable B_r responds to changes in model parameters. This analysis helps pinpoint which parameters of B_r significantly influence observed outcomes.

7.1. **Definition (Normalized forward sensitivity index).** The normalized forward sensitivity index of B_r regards to the defined parameter Π is given by [12],

$$S_{\Pi} = \left(\frac{\partial B_r}{\partial \Pi}\right)\left(\frac{\Pi}{B_r}\right).$$

In order to assess sensitivity indices, various methodologies can be employed, including the linearization method, Latin hypercube sampling, and the direct differentiation method. The outcomes from each approach can be analyzed to understand the system's sensitivity. In this study, we specifically employed the direct differentiation method. These sensitivity indices offer insights about which parameters positively or negatively impact the system, which in turn helps in formulating effective disease management policies. In Table 1, it is observed that ς, Π, ξ, and q_1 positively influence B_r, as indicated. Conversely, $\sigma, \Theta, q_2, d, n_1$, and n_2 have a negative impact on B_r. Changes in these parameter values lead to either an increase or a decrease in B_r. For instance, a 10% increase in these parameters results in approximately $9.99\%, 10\%, 0.0523\%, 7.1795\%$ increase in B_r, as shown in Table 1. Conversely, there is an approximate decrease of $17.4058\%, 0.1408\%, 3.5081\%, 9.948\%, 6.1582\%, 10\%$ in the value of B_r if adjustments are made to the indices for parameters $S_{\Theta}, S_{n_1}, S_{n_2}, S_d, S_{q_2}, S_{\sigma}$.

TABLE 2. Sensitivity Results.

Parameters	S.index	Values	Parameters	S.index	Values
ς	S_ς	0.9984525824	Π	S_Π	0.9999999990
ξ	S_ξ	0.005231744158	σ	S_σ	-1.740577486
Θ	S_Θ	-0.01408450704	q_1	S_{q_1}	0.7179594473
q_2	S_{q_2}	-0.3508133672	d	S_d	-0.9947682551
n_1	S_{n_1}	-0.6158277582	n_2	S_{n_2}	0

(a)   (b)
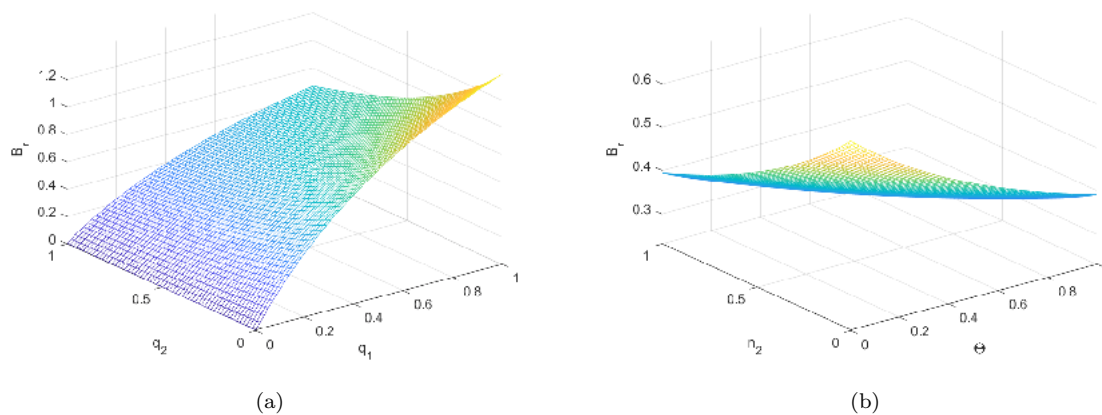
FIGURE 1. (a)Behaviour of B_r against q_1 and q_2, (b) Behaviour of B_r against n_2 and Θ.

(a)   (b)
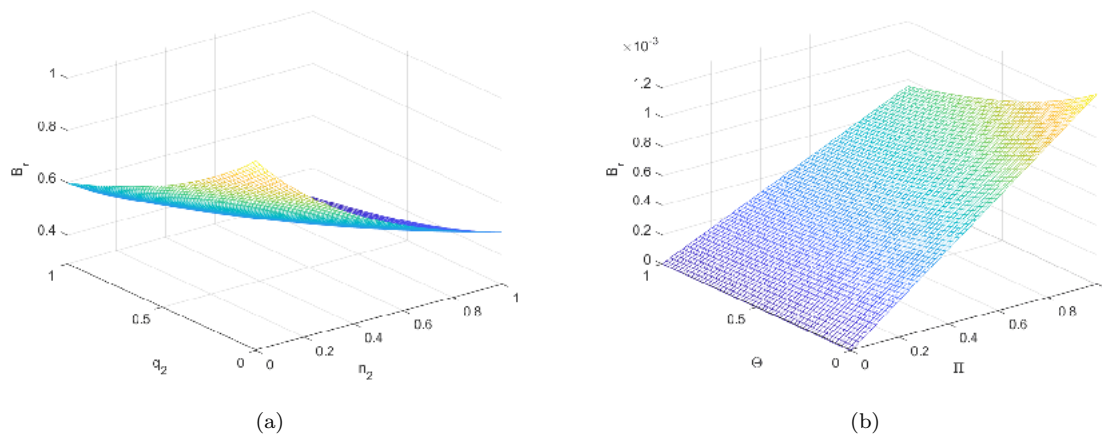
FIGURE 2. (a)Behaviour of B_r against q_2 and n_2, (b) Behaviour of B_r against Θ and Π.

8. PRCC TEST

To explore the relationships among the parameters of (4.1), Latin hypercube sampling (LHS) is utilized, a method for creating random parameter sets that comprehensively sample the variable space [2, 22, 28]. We analyzed the
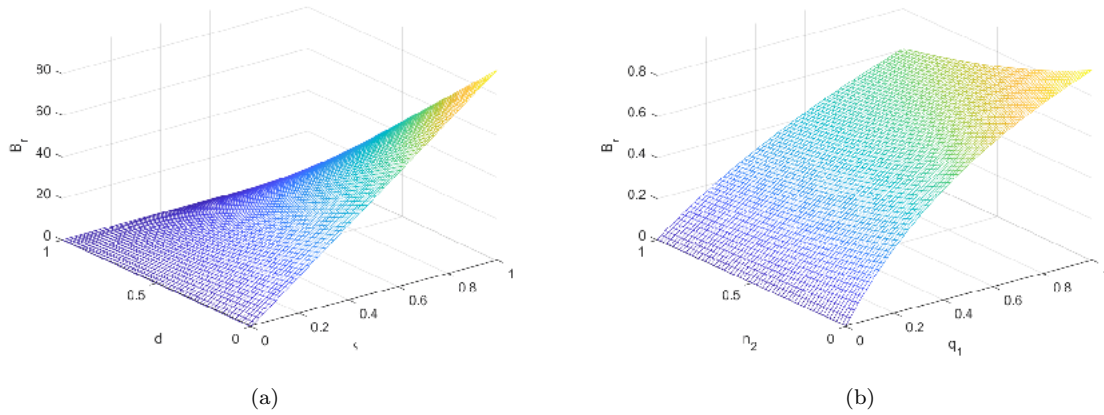
FIGURE 3. (a)Behaviour of B_r against d and ς, (b)Behaviour of B_r against n_2 and q_1.
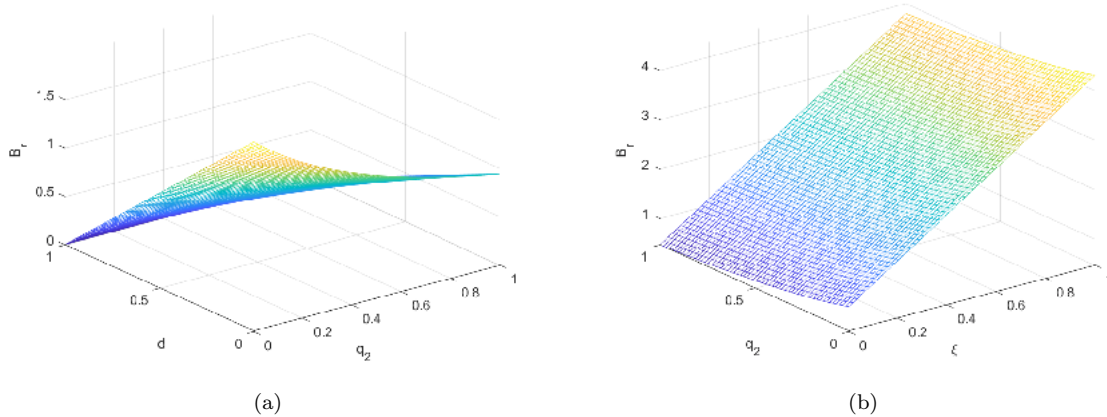

FIGURE 4. (a) Behaviour of B_r against d and q_2, (b)Behaviour of B_r against q_2 and ξ.

uncertainty in model parameters using LHS sampling in conjunction with partial rank correlation coefficients (PRCCs) [25].

Each uncertain variable is assumed to follow a uniform distribution whitin a certain range, usually $\pm 30\%$ of its reference point. A LHS analysis was performed by drawing 1000 random samples from these parameter distributions. Afterwards, PRCCs were computed for each of the specified parameters $(\Pi, \xi, \varsigma, \sigma, \gamma, d, q_1, q_2, n_1, n_2)$ in relation to the outcome variable, the (B_r). The direction of the PRCCs signifies whether changes in the input parameters have a positive or negative impact on the related output variable. The most significant variables are those with PRCC results satisfying $|PRCC| > 0.4$, with a negative sign indicating an inverse relationship. A correlation between the output variable and the input variables is considered moderate if $0.2 < |PRCC| < 0.4$, and weak otherwise [26]. Figure 7 highlights that the parameters "$\Pi, \varsigma, n_1, q_1, n_2, q_2$" have a major consequence on the outcome function, specifically the reproduction number (B_r).

Conversely, the parameters "ξ, d, σ, Θ" demonstrate an insignificant impact on B_r. Contagion rate (ς) is a principal factors that contribute to inflation in B_r. Variables that result in a decrease in B_r include the proportion of exposed
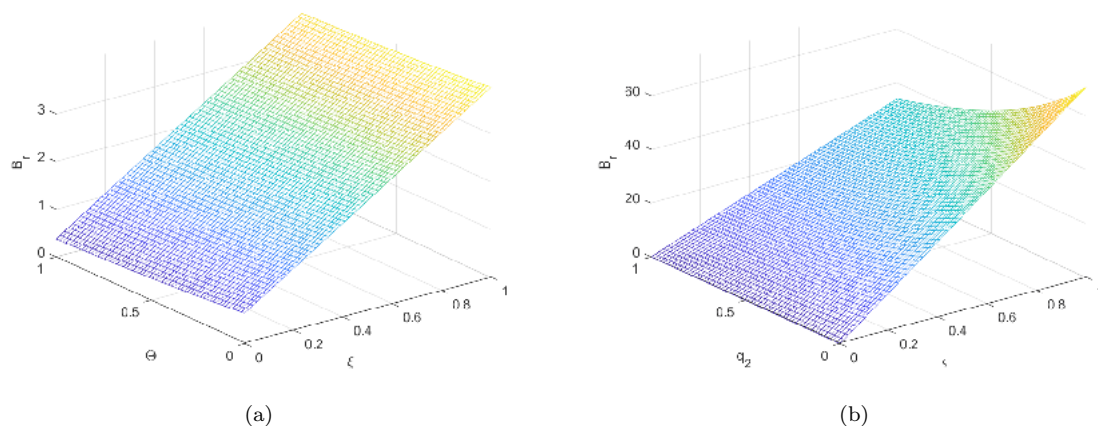
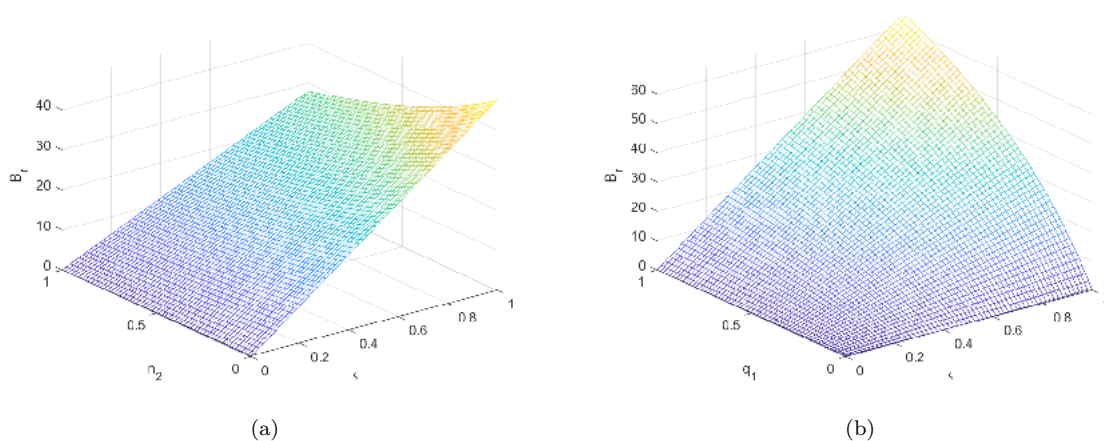FIGURE 5. (a) Behaviour of B_r against Θ and ξ, (b)Behaviour of B_r against q_2 and ς.

FIGURE 6. (a)Behaviour of B_r against n_2 and ς, (b)Behaviour of B_r against q_1 and ς.

individuals developing infections (ξ), the restoration frequency of infectious individuals (q_2), the death frequency of infectious individuals (σ), q_2 is the rate of transmission moved from infectious position to the recovered position and vaccination rate for susceptible and exposed are (n_1) and (n_2), respectively.

9. NUMERICAL SCHEME FOR THE SEIR MODEL USING ATANGANA-BALEANU-CAPUTO DERIVATIVE

Let us now examine the scheme utilizing the Atangana-Baleanu-Caputo derivative (Atangana Toufik method) [27]. We will use this scheme for simulating our SEIR fractional derivative model (4.1) as follows:

$$\mathcal{S}_{p+1} = \mathcal{S}_0 + \frac{1-\eta}{\mathcal{ABC}(\eta)}\psi_1(t_p, A(t_p)) + \frac{\eta}{\mathcal{ABC}(\eta)}\sum_{r=0}^{k}\left[\frac{h^\eta\psi_1(t_r, A_r)}{\Gamma(\eta+2)}((\eta-r+k+2)(1-r+k)^\eta\right.$$
$$\left. - (2\eta-r+2+k)(-r+k)^\eta) - \frac{h^\eta\psi_1(t_{r-1}, A_{r-1})}{\Gamma(\eta+2)}(-(-r+k)^\eta(\eta-r+1+k)+(1-r+k)^{\eta+1})\right],$$
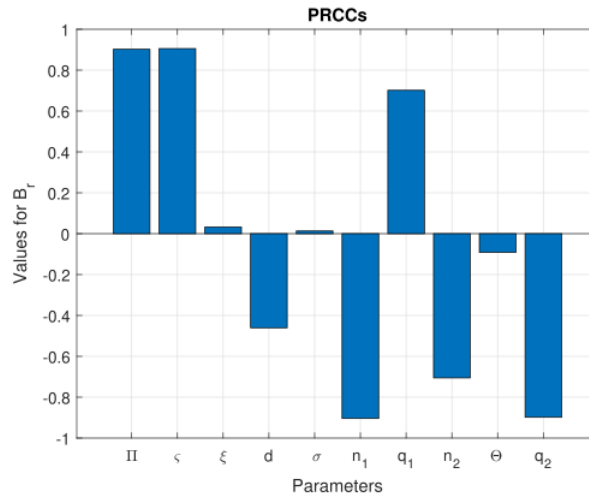
FIGURE 7. PRCCs test results, demonstrate how the model parameters influence the dependence of B_r.

TABLE 3. Realistic values of parameters.

Variables	Values	variables	Values
σ	[DFE: 0.9, EE: 0.001]	ς	0.0139
ξ	0.001	Π	500
d	0.5	n_1	0.5
n_2	0.5	Θ	0.02
q_1	0.54	q_2	0.5

$$\mathcal{E}_{p+1} = \mathcal{E}_0 + \frac{1-\eta}{\mathcal{ABC}(\eta)}\psi_2(t_p, A(t_p)) + \frac{\eta}{\mathcal{ABC}(\eta)}\sum_{r=0}^{k}\left[\frac{h^\eta\psi_2(t_r, A_r)}{\Gamma(\eta+2)}((\eta-r+k+2)(1-r+k)^\eta\right.$$
$$\left. - (2\eta-r+2+k)(-r+k)^\eta) - \frac{h^\eta\psi_2(t_{r-1}, A_{r-1})}{\Gamma(\eta+2)}(-(-r+k)^\eta(\eta-r+1+k)+(1-r+k)^{\eta+1})\right],$$

$$\mathcal{I}_{p+1} = \mathcal{I}_0 + \frac{1-\eta}{\mathcal{ABC}(\eta)}\psi_3(t_p, A(t_p)) + \frac{\eta}{\mathcal{ABC}(\eta)}\sum_{r=0}^{k}\left[\frac{h^\eta\psi_3(t_r, A_r)}{\Gamma(\eta+2)}((\eta-r+k+2)(1-r+k)^\eta\right.$$
$$\left. - (2\eta-r+2+k)(-r+k)^\eta) - \frac{h^\eta\psi_3(t_{r-1}, A_{r-1})}{\Gamma(\eta+2)}(-(-r+k)^\eta(\eta-r+1+k)+(1-r+k)^{\eta+1})\right],$$

$$\mathcal{R}_{p+1} = \mathcal{R}_0 + \frac{1-\eta}{\mathcal{ABC}(a)}\psi_4(t_p, A_p)) + \frac{\eta}{\mathcal{ABC}(\eta)}\sum_{r=0}^{k}\left[\frac{h^a\psi_4(t_r, A_r)}{\Gamma(\eta+2)}((\eta-r+k+2)(1-r+k)^\eta\right. \tag{9.1}$$
$$\left. - (2\eta-r+2+k)(-r+k)^\eta) - \frac{h^\eta\psi_4(t_{r-1}, A_{r-1})}{\Gamma(\eta+2)}(-(-r+k)^\eta(\eta-r+1+k)+(1-r+k)^{\eta+1})\right].$$

10. CONCLUSIONS

This research investigates the utilization of fractional-order derivatives employing the ABC operator, where the fractional order is confined within the range $0 < \eta \leq 1$, applied to the SEIR model. We computed the approximate
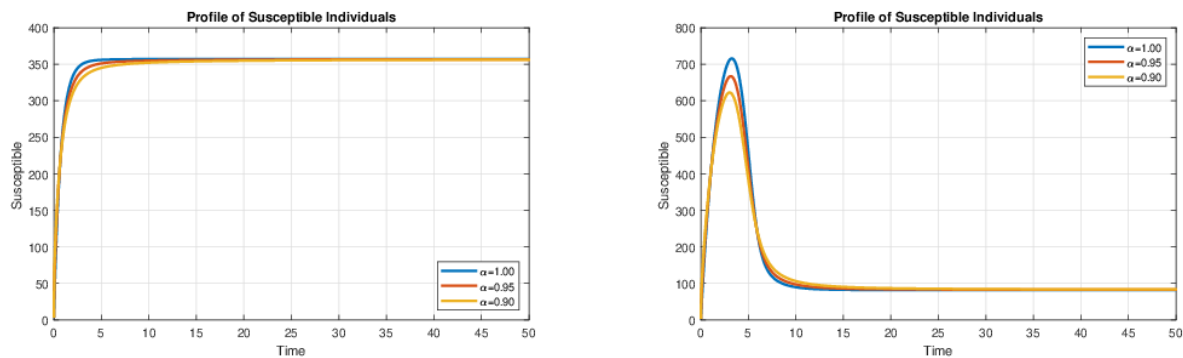
FIGURE 8. Numerical solutions of the system (4.1) using fractional order ABC derivative with $\mathcal{S}_f = 357.1429, \mathcal{S}_p = 144.2357$. Left: The susceptible profile $\mathcal{S}(\mathfrak{t})$ for D_f is shown on the left side using the ABC fractional derivative, while the susceptible profile $\mathcal{S}(\mathfrak{t})$ for D_p is displayed on the right side using the ABC fractional derivative.
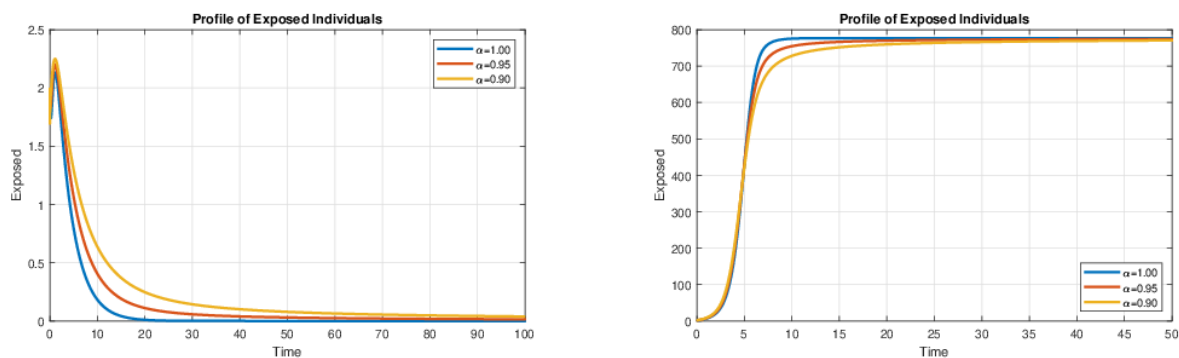

FIGURE 9. Numerical solutions of system (4.1) utilizing fractional order ABC derivative, with $\mathcal{E}_f = 0$ and $\mathcal{E}_p = 410.8914$. Left: The exposed profile $\mathcal{E}(\mathfrak{t})$ for D_f is depicted on the left side, employing the ABC fractional derivative, while the exposed profile $\mathcal{E}(\mathfrak{t})$ for D_p is presented on the right side using the ABC fractional derivative.
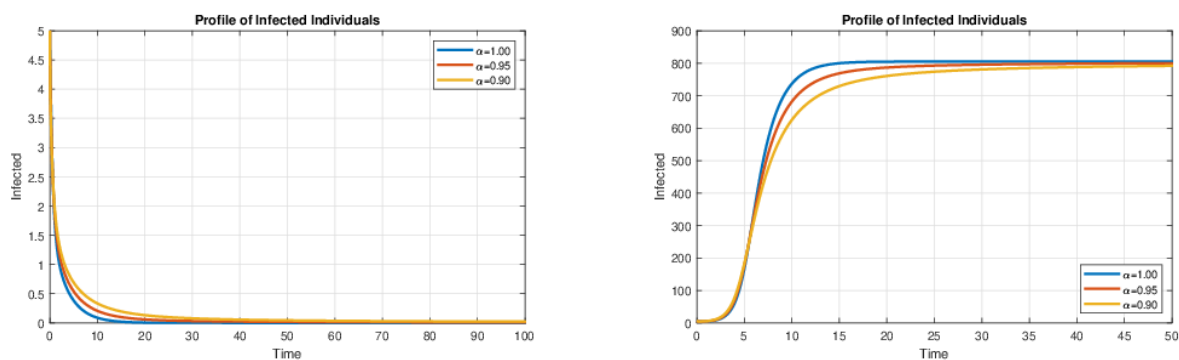

FIGURE 10. Numeric solutions for system (4.1) are obtained using a fractional order ABC derivative with $\mathcal{I}_f = 0$ and $\mathcal{I}_p = 425.8759$. On the left, the infected profile $\mathcal{I}(\mathfrak{t})$ for D_f is shown utilizing the ABC fractional derivative, while on the right, the infected profile $\mathcal{I}(\mathfrak{t})$ for D_p is depicted using the ABC fractional derivative.
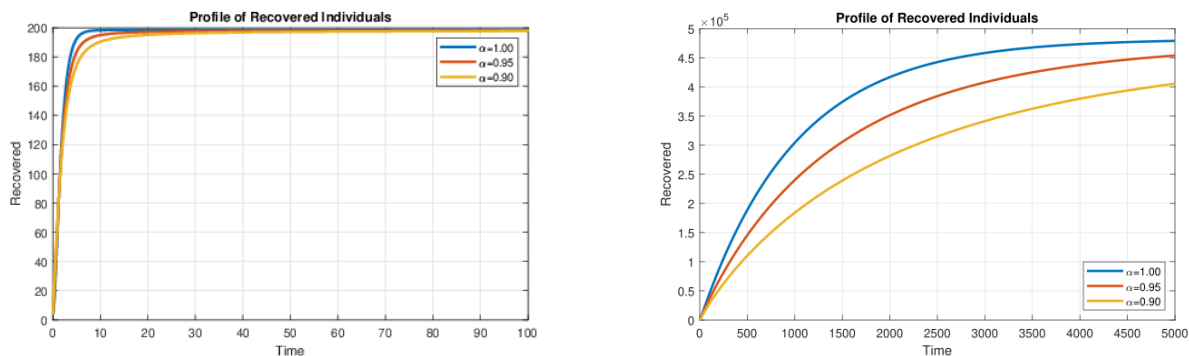
FIGURE 11. Numerical solutions for system (4.1) are obtained using a fractional-order ABC derivative with $\mathcal{R}_f = 198.4127$ and $\mathcal{R}_p = 4.9050 * 10^5$. On the left, the recovered profile $\mathcal{R}(t)$ for D_f is depicted utilizing the ABC fractional derivative, while on the right, the recovered profile $\mathcal{R}(t)$ for D_p is illustrated using the ABC fractional derivative.

values of B_r as 0.4891 in the case of an infection-free scenario and 6.9193 for the endemic scenario. Global stability of stable points was demonstrated by constructing a Lyapunov function. We established the existence and uniqueness of global positive solutions. Specifically, we verified both local and global infection-free stable points for $B_r < 1$, and the condition for an endemic stable point is $B_r > 1$. The utilization of fractional-order derivatives in modeling provides improved efficiency compared to integer-order derivatives, attributed to the flexibility in selecting derivative orders that offer an additional degree of freedom.

Availability of Data

None.

Declaration of interests

None.

Acknowledgment

None.

References

[1] Z. Abbasi, I. Zamani, A. H. A. Mehra, M. Shafieirad, and A. Ibeas, *Optimal control design of impulsive SQEIAR epidemic models with application to COVID-19*, Chaos Solitons Fractals, *139* (2020), 110054.

[2] F. B. Agusto, E. Numfor, K. Srinivasan, E. A. Iboi, A. Fulk, and J. M. Saint Onge, A. T. Peterson, *Impact of public sentiments on the transmission of COVID-19 across a geographical gradient*, PeerJ, *11* (2023), e14736.

[3] R. T. Alqahtani, *Atangana-Baleanu derivative with fractional order applied to the model of groundwater within an unconfined aquifer*, J. Nonlinear Sci. Appl., *9* (2016), 3647–3654.

[4] J. Arino, F. Brauer, P. van den Driessche, J. Watmough, and J. Wu, *A model for influenza with vaccination and antiviral treatment*, J. Theor. Biol., *253* (2008), 118–130.

[5] I. A. Baba, E. Hincal, and S. H. K. Alsaadi, *Global stability analysis of a two strain epidemic model with awareness*, Adv. Differ. Equ. Control Processes, *19* (2018), 83–100.

[6] D. Baleanu, A. Jajarmi, and M. Hajipour, *On the nonlinear dynamical systems within the generalized fractional derivatives with Mittag–Leffler kernel*, Nonlinear Dyn., *94* (2018), 397–414.

[7] A. Basit, M. Tufail, M. Rehan, and I. Ahmed, *A new event-triggered distributed state estimation approach for one-sided Lipschitz nonlinear discrete-time systems and its application to wireless sensor networks*, ISA Trans., *137* (2023), 74–86.

[8] M. A. Bayrak, A. Demir, and E. Ozbilge, *On solution of fractional partial differential equation by the weighted fractional operator*, Alex. Eng. J., *59* (2020), 4805–4819.

[9] E. Bonyah, H. S. Panigoro, E. Rahmi, and M. L. Juga, *Fractional stochastic modelling of monkeypox dynamics*, Results in Control and Optimization, *12* (2023), 100277.

[10] S. K. Brooks, R. K. Webster, L. E. Smith, L. Woodland, S. Wessely, N. Greenberg, and G. Rubin, *The psychological impact of quarantine and how to reduce it: rapid review of the evidence*, The Lancet, *395* (2020), 912–920.

[11] A. I. K. Butt, W. Ahmad, M. Rafiq, and D. Baleanu, *Numerical analysis of Atangana-Baleanu fractional model to understand the propagation of a novel corona virus pandemic*, Alex. Eng. J., *61* (2022), 7007–7027.

[12] P. V. Den Driessche and J. Watmough, *Reproduction numbers and sub-threshold endemic equilibria for compartmental models of disease transmission*, Math. Biosci., *180* (2002), 29–48.

[13] M. El Fatini, I. Sekkak, and A. Laaribi, *A threshold of a delayed stochastic epidemic model with Crowly–Martin functional response and vaccination*, Physica A, *520* (2019), 151–160.

[14] P. Gahinet and P. Apkarian, *A linear matrix inequality approach to H_∞ control*, Int. J. Robust Nonlinear Control, *4* (1994), 421–448.

[15] M. Iannelli, M. Martcheva, and X. Z. Li, *Strain replacement in an epidemic model with super-infection and perfect vaccination*, Math. Biosci., *195* (2005), 23–46.

[16] S. A. Jose, R. Ramachandran, D. Baleanu, H. S. Panigoro, J. Alzabut, and V. E. Balas, *Computational dynamics of a fractional order substance addictions transfer model with Atangana–Baleanu–Caputo derivative*, Math. Methods Appl. Sci., *46* (2023), 5060–5085.

[17] N. Leung, D. K. Chu, E. Y. Shiu, K. Chan, J. J. McDevitt, B. J. Hau, H. Yen, Y. G. Li, D. K. Ip, J. Peiris, W. Seto, G. M. Leung, D. K. Milton, and B. J. Cowling, *Respiratory virus shedding in exhaled breath and efficacy of face masks*, Nat. Med., *26* (2020), 676–680.

[18] Q. Liu and Q. M. Chen, *Analysis of the deterministic and stochastic SIRS epidemic models with nonlinear incidence*, Physica A, *428* (2015), 140–153.

[19] Q. Liu, D. Jiang, T. Hayat, and A. Alsaedi, *Dynamics of a stochastic predator–prey model with distributed delay and Markovian switching*, Physica A: Stat. Mech. Appl., *527* (2019), 121264.

[20] X. Z. Li, J. Wang, and M. Ghosh, *Stability and bifurcation of an SIVS epidemic model with treatment and age of vaccination*, Appl. Math. Model., *34* (2010), 437–450.

[21] G. P. Matthews and R. A. De Carlo, *Decentralized tracking for a class of interconnected nonlinear systems using variable structure control*, Automatica, *24* (1988), 187–193.

[22] S. Marino, I. B. Hogue, C. J. Ray, and D. E. Kirschner, *A methodology for performing global uncertainty and sensitivity analysis in systems biology*, J. Theor. Biol., *254* (2008), 178–196.

[23] A. Mehra, I. Zamani, Z. Abbasi, and A. Ibeas, *Observer-based adaptive PI sliding mode control of developed uncertain SEIAR influenza epidemic model considering dynamic population*, J. Theor. Biol., *482* (2019), 118–130.

[24] P. W. Nelson, M. A. Gilchrist, D. Coombs, J. M. Hyman, and A. S. Perelson, *An age-structured model of HIV infection that allows for variations in the production rate of viral particles and the death rate of productively infected cells*, Math. Biosci. Eng., *1* (2004), 267–288.

[25] A. T. Peterson, A. Fulk, E. Numfor, E. A. Iboi, F. B. Agusto, J. M. Saint Onge, and K. Srinivasan, *Impact of public sentiments on the transmission of COVID-19 across a geographical gradient*, PeerJ, *11* (2023), e14736.

[26] A. J. E. M. Saltelli, D. Cariboni, J. Gatelli, and R. Liska, *The role of sensitivity analysis in ecological modelling*, Ecol. Model., *203*(1–2) (2007), 167–182.

[27] M. Toufik and A. Atangana, *New numerical approximation of fractional derivative with non-local and non-singular kernel: application to chaotic models*, Eur. Phys. J. Plus, *132* (2017), 1–16.

[28] Y. Wang, Y. Zhou, F. Brauer, and J. M. Heffernan, *Viral dynamics model with CTL immune response incorporating antiretroviral therapy*, J. Math. Biol., *67* (2013), 901–934.

[29] Y. Wang, J. Liu, and J. M. Heffernan, *Viral dynamics of an HTLV-I infection model with intracellular delay and CTL immune response delay*, J. Math. Anal. Appl., *459*(1) (2018), 506–527.

[30] Y. Wang, J. Liu, and L. Liu, *Viral dynamics of an HIV model with latent infection incorporating antiretroviral therapy*, Adv. Differ. Equ., *2016* (2016), 1–15.

[31] D. M. Xiao and S. G. Ruan, *Global analysis of an epidemic model with nonmonotone incidence rate*, Math. Biosci., *208* (2007), 419–429.

[32] X. Zhang, D. Jiang, T. Hayat, and B. Ahmad, *Dynamics of a stochastic SIS model with double epidemic diseases driven by Lévy jumps*, Physica A: Stat. Mech. Appl., *471* (2017), 767–777.